

## ORIGINAL CONTRIBUTION

# Role of Autophagy and Apoptosis in Wound Tissue of Deep Second-degree Burn in Rats

Mengjing Xiao, MD, Ligen Li, MD, Chenxi Li, MD, Peirong Zhang, RN, Quan Hu, MD, Li Ma, PhD, and Haijun Zhang, MD

### Abstract

**Objectives:** The pathogenesis of burn wound progression is poorly understood. Contributing factors include continuous loss of blood perfusion, excessive inflammation, and elevated apoptosis levels in wound tissue. Macroautophagy (here referred to simply as “autophagy”) is associated with many chronic diseases. The authors hypothesized that autophagy is involved in burn wound progression in a rat model of deep second-degree burn.

**Methods:** Deep second-degree burns were modeled using a brass rod heated to 100°C applied for 6 seconds to the back skin of Wistar rats. Full-thickness biopsies were obtained from burned and nonburned controls at several times postburn. Western blotting and immunohistochemical (IHC) staining determined expression of the autophagy markers Light Chain 3 (LC3) and beclin-1. Apoptosis was determined by terminal-deoxynucleotidyl transferase mediated nick end labeling (TUNEL) assay and laser Doppler flowmetry (LDF)-measured tissue perfusion. Myeloperoxidase (MPO) activity assay measured inflammation. Hematoxylin and eosin (H&E) and Masson’s trichrome staining-determined pathology and wound depth.

**Results:** The LC3 and beclin-1 protein level in burn wounds decreased to one-fourth of normal levels ( $p < 0.01$ ) over 24 hours and then began to increase but still did not reach their normal level. TUNEL-positive cells in burn wounds were 3.7-fold ( $p < 0.01$ ) elevated over 48 hours and then decreased slightly, yet still remained higher than in normal skin. The burn wound progressed in depth over 72 hours. In addition, significant decrease in LDF values and upregulation of MPO activity were observed. Enhanced LC3-positive cells were observed in the deep dermal layer of burn wounds as shown by IHC staining.

**Conclusions:** A reduction in autophagy and blood flow and an increase in apoptosis and inflammation were observed in burn wounds early during the course of burn injury progression. This suggests that autophagy, complemented by apoptosis, play important roles in burn progression. Enhanced autophagy in the deep dermis may be a prosurvival mechanism against ischemia and inflammation after burn injury.

ACADEMIC EMERGENCY MEDICINE 2014;21:383–391 © 2014 by the Society for Academic Emergency Medicine

**B**urn wound progression is a widely acknowledged pathophysiologic process that often occurs within 72 hours after a burn.<sup>1</sup> The progression of burn wounds makes treatment more difficult, prolongs hospital stay, increases costs, and increases the likelihood of scarring. For these reasons, it is of great significance to prevent burn wound progression. A number of mechanisms are thought to be involved in the process of burn wound progression, including local tissue hypoperfusion, edema, prolonged inflammation, hypercoagulability, free radical damage, and accumulation of cytotoxic cytokines.<sup>1–3</sup> Many attempts have been made to prevent burn wound pro-

gression by modulating these mechanisms. However, further study is still needed to better understand this process.

Recently studies<sup>2</sup> have suggested that cell death may occur as a result of three distinct pathways, including necrosis, apoptosis, and autophagy, all of which may lead to further burn injury progression. Studies have shown that apoptosis and necrosis are both involved in burn wound progression,<sup>4,5</sup> and it has been demonstrated<sup>5</sup> that apoptosis is one of the contributing factors of burn wound progression. Inhibiting apoptosis reduces continuous tissue loss and promotes burn wound healing.<sup>6,7</sup> However, to date, little is known

From the Department of Burn and Plastic Surgery, Burn Institute First Affiliated Hospital of General Hospital of PLA (MX, LL, CL, QH, LM, HZ), Beijing, China; and the Hematology Department, Beijing Daopei Hospital (PZ), Beijing, China.

Received April 13, 2013; revisions received July 11, September 11, and September 22, 2013; accepted October 31, 2013.

The authors have no relevant financial information or potential conflicts of interest to disclose.

Supervising Editor: James E. Olson, PhD.

Address for correspondence and reprints: Li Ligen, MD; e-mail: liligen@126.com.

about the relationship between autophagy and burn wound progression.

Autophagy<sup>8,9</sup> is a highly conserved pathway that delivers intracellular macromolecule waste to lysosomes, where they are degraded into biologically active monomers, such as amino acids, that are subsequently reused to maintain cellular metabolic turnover and homeostasis. Autophagy is linked to apoptosis in many ways, yet their roles in the pathogenesis of burn wounds remain unclear. This study was designed to determine whether there were changes in autophagy and apoptosis in a deep second-degree rodent burn model and to explore the association between these changes and wound progression.

## METHODS

### Study Design

This was a laboratory study of burn wound progression in the murine model. The experimental protocol was approved by the Institutional Animal Care & Use Committee of First Hospital Affiliated to PLA General Hospital.

### Animal Handling and Preparation

Experiments were performed on 56 male Wistar rats weighing 200 to 220 grams. Animals were housed for at least 7 days prior to experiments in a ventilated and temperature-controlled room and had access to water ad libitum.

Anesthesia was performed by intramuscular injection of 100 mg/kg ketamine (Gutian Pharmaceutical Co., LTD, Fujian, China) and 25 mg/kg xylazine hydrochloride (Dunhua Animal Pharmaceutical Co., LTD, Jilin, China). The hair on the dorsal skin of the rats was removed by electric clippers. A 1.8-cm-diameter brass rod with a height of 3 cm, and a weight of 200 g was heated to 100°C and applied to the skin for 6 seconds to produce a deep second-degree burn as previously described.<sup>10</sup> Only the weight of the rod was used to create the burns; no additional pressure was placed on it. To avoid variations in creating the burns, one person created all burns. Three burns were created on each half of the dorsal skin at 1 cm apart. Six burns (10% total body surface area, approximately) were created on each animal. The temperature of the brass rod was regulated by a temperature controller and varied by <1°C during the process of thermal injury. The burn depth was confirmed by two experienced histopathologists and, by microscopic examination, showed destruction of hair follicles and vessel walls, microthrombi, and neutrophils in the deep dermis, yet a few hair follicles remained.

### Study Protocol

**Animal Grouping and Tissue Preparation.** The rats were randomly divided into six time points (eight rats at each time point) to assess postburn endpoints at 1, 6, 12, 24, 48, and 72 hours. Eight healthy adult rats without burns were used as controls. The control group was assumed to be unchanged over the time course of the investigation. The data from the control group were used for multiple comparisons with the experimental

groups at each time point. After laser Doppler flowmetry (LDF) values were measured, the rats were euthanized. All skin/wound samples were collected and sorted by the number of rats; in other words, the eight samples in each time point were from eight different rats. The samples were subjected to hematoxylin and eosin (H&E), Masson's trichrome staining (Masson staining), terminal-deoxynucleotidyl transferase mediated nick end labeling (TUNEL) assay, and immunohistochemical (IHC) staining. The other parts of the specimen were homogenized for myeloperoxidase (MPO) activity assay and Western blot analysis.

**Western Blot Analysis.** Western blot analysis was employed to determine the protein levels of two autophagy markers, Light Chain 3 (LC3) and beclin-1. Expression of these markers reflected autophagy levels in burn wounds. The autophagy marker LC3 was originally identified as a subunit of microtubule-associated proteins 1A and 1B and was subsequently found to display similarity to the yeast protein Apg8/Aut7/Cvt5, which is critical for autophagy.<sup>11</sup> Cleavage of LC3 at the carboxy terminus immediately following synthesis yields the cytosolic LC3-I form. During autophagy, LC3-I is converted to LC3-II through lipidation (the covalent binding of a lipid group to a peptide chain) by an ubiquitin-like system involving Atg7 and Atg3 that allows LC3 to become associated with autophagic vesicles.<sup>12</sup> The ratio of LC3-II/LC3-I has been used as an indicator of autophagy.<sup>13</sup> Beclin-1, the mammalian ortholog of the yeast autophagy protein Apg6/Vps30, is one of the proteins critical to autophagy.<sup>14</sup> The level of beclin-1 was also an indicator of autophagy.<sup>15</sup>

The skin/wound samples were cut into small pieces and homogenized (DIAX 900, Heidolph, Schwabach, Germany; 4°C, at 25,000 rpm, for 5 minutes) in lysis buffer containing 50 mmol/L Tris HCl (pH 7.6), 20 mmol/L MgCl<sub>2</sub>, 150 mmol/L NaCl, 0.5% Triton-X, 5 units/mL aprotinin, 5 µg/mL leupeptin, 5 µg/mL pepstatin, 1 mmol/L benzamidine, and 1 mmol/L phenylmethylsulfonyl fluoride. The debris was removed by centrifugation, and the protein levels in the lysates were determined by bicinchoninic acid protein assay kit (Pierce Biotechnology, Rockford, IL). Protein (50 µg) in the lysates was separated using sodium dodecyl sulfate-polyacrylamide 15% gel electrophoresis and electrophoretically transferred to a polyvinylidene difluoride membrane. The membranes were blocked for 2 hours at room temperature in Tris-buffered saline with Tween (TBST) buffer (0.01 mol/L Tris-HCl, pH 7.5, 0.15 mol/L NaCl, and 0.05% Tween 20) containing 5% skimmed milk. They were then incubated with rabbit anti-LC3 antibodies (1:500, Cell Signaling Technology, Boston, MA) and anti-beclin-1 antibodies (1:500, Cell Signaling Technology) diluted in TBST buffer overnight at 4°C. The membranes were washed three times and incubated for 1 hour at room temperature with secondary antibody linked to horseradish peroxidase (1:2000; Invitrogen, Carlsbad, CA). Immunoreactive bands were developed using an enhanced chemiluminescence reagent (Pierce Biotechnology) and exposed onto Kodak film (Eastman Kodak, Rochester, NY). Band densities were normalized using glyceraldehyde-3-phosphate

dehydrogenase and quantified using a scanning densitometric analysis Image J software (National Institutes of Health, Bethesda, MD).

**Immunohistochemical Staining of LC3.** In addition to Western blot assay, we performed IHC staining of LC3 to be supplemented with visualized images. Samples were fixed in 10% neutralized formalin, embedded in paraffin, and sectioned by a slicing machine (Leica Microsystems, Wetzlar, Germany). Serial sections (5  $\mu$ m) were deparaffinized, rehydrated, and washed in phosphate-buffered saline (PBS) for 10 minutes and then incubated in hydrogen peroxide block for 10 minutes. This was followed by washing with PBS containing 0.3% Tween for 10 minutes and blocking with 3% milk and 5% fetal bovine serum in 0.01 mol/L PBS for 2 hours. The sections were incubated with rabbit anti-LC3 antibodies (1:100; Cell Signaling Technology) diluted in PBS overnight at 4°C. After being rinsed with PBS, the sections were incubated with goat anti-rabbit secondary antibody (1:500; Boster, Wuhan, China) for 1 hour at room temperature. Since LC3 is expressed in the cytoplasm, cells staining blue in their nuclei and brown in their cytoplasm were considered positive. The sections were observed under a light microscope at 400  $\times$  magnification. The investigators were blinded to the animal grouping. Slices were photographed continuously and nonoverlapping from left to right, up to down. Pictures were numbered and random fields were obtained by random number method generated by computer. The final value of a slice was obtained by a mean value from at least six random high-power fields. Quantitative analysis was performed using Image-Pro Plus 6.0 software (Media Cybernetics, Rockville, MD) and integrated optical density was computed for statistical analysis.

**TUNEL Staining to Examine Apoptosis in Wound Tissue.** To investigate the apoptosis level of burn wounds, we conducted TUNEL staining to see how the apoptosis level in burn wounds would change after the burns were inflicted. The TUNEL staining assay kit (Roche Diagnostics, Penzberg, Germany) and all associated procedures were performed according to the manufacturer's instruction booklet for the in situ cell death detection kit. Briefly, samples were fixed in 10% neutralized formalin and embedded in paraffin. Serial sections were deparaffinized, rehydrated, and incubated for 20 minutes at 37°C with proteinase K working solution (15  $\mu$ g/mL in 10 mmol/L Tris-HCl, pH 7.5). After being rinsed twice with PBS, slices were incubated in hydrogen peroxide block for 10 minutes, and then 50- $\mu$ L TUNEL reaction mixtures were added on the slices. Slices were incubated for 60 minutes at 37°C in a humidified atmosphere in the dark. After being rinsed with PBS, slices were added to 50  $\mu$ L of converter-peroxidase and incubated in a humidified chamber for 30 minutes at 37°C, and then 50  $\mu$ L of diaminobenzidine substrates was added and the slices were incubated for 10 minutes at 25°C. After being rinsed with PBS, slices were analyzed under a light microscope. Cells with shrunken brown-stained nuclei were considered positive. The investigators were blinded to the animal grouping. Slices were photographed continuously and

nonoverlapping from left to right, up to down. Pictures were numbered and random fields were obtained by random number method generated by computer. The apoptotic rate was obtained by counting the TUNEL-positive cells compared to all the visible cells at a 400  $\times$  magnification. A mean value was calculated from at least eight values and the final values were subjected to statistical analysis.

**H&E and Masson Staining.** H&E and Masson staining were performed to evaluate the histopathologic changes of burn wounds. Masson staining was also designed to show the extent of tissue necrosis progressed over time. The assay kits were purchased from Fuzhou Maixin Bioengineering Institute (Fujian, China). For H&E staining, sections were deparaffinized and rehydrated. After slices were washed and dried, hematoxylin was added for 5 minutes; after rinsing with water, 1% HCl alcohol solution was added for 10 seconds. Slices were washed for 25 minutes, 0.5% eosin was added for 2 minutes, and then slices were dehydrated with 95% and 100% ethanol. Dimethylbenzene was added for 5 minutes, twice. Slices were observed under a light microscope. For Masson staining, sections were deparaffinized, rehydrated, and incubated in hematoxylin iron solution for 10 minutes. Hydrochloric acid alcohol was added for 1 minute and then slices were washed for 25 minutes. Acid fuchsin solution was added for 8 minutes and 1% phosphomolybdic acid for 5 minutes. After that, slices were incubated with aniline blue for 5 minutes, and 1% glacial acetic acid was added for 1 minute. Slices were then dehydrated in 95% and 100% ethanol and transparentized in dimethylbenzene. Slices were observed under a light microscope.

**Detection of LDF Value in the Wound Tissue.** Laser Doppler flow values in burn wounds were an indicator of burn wound blood flow.<sup>10</sup> We designed the LDF assay to observe the blood flow changes in burn wounds over time and its potential link with the changes of autophagic levels in the process of burn wound progression. For measurement of LDF, the rats were anaesthetized using the same protocol as in the experimental model. LDF was measured with a commercial Periflux 5000 probe 404 device (Perimed, Stockholm, Sweden). LDF was measured according to the instructions of the product specification booklet as provided by the company. Briefly, specialized double-faced adhesive tape was used to bond the probe and rat skin and the perfusion unit value was read by the computer. Each wound was trisected horizontally and vertically, so nine partitions were established. Random samples were obtained by random number method generated by computer. The final perfusion unit value of a burn wound was obtained by a mean value from at least six random perfusion unit values within the wound. The room temperature was maintained at 23°C (SD  $\pm$  1°C) and the humidity was 45% (SD  $\pm$  3%).

**Detection of MPO Activity in Wound Tissue.** Myeloperoxidase activity reflects the inflammatory response in the burn wound.<sup>10</sup> We performed this assay to determine the changes in inflammatory infiltration of the

burn wound over time and its potential link with the changes of autophagic levels in the process of burn wound progression. Determination of MPO activity in the burn wound tissue specimens was assayed according to a commercial kit and the manufacturer's instructions (Nanjing Jiancheng Bioengineering Institute, Jiangsu, China). Briefly, fresh tissue samples (100 mg) were homogenized on ice in 500  $\mu$ L of PBS, pH 7.4, containing 0.1% Tween 20. Subsequently, samples were centrifuged at  $16,000 \times g$  at  $4^{\circ}\text{C}$  for 10 minutes. Supernatants were stored on ice for immediate analysis. Twenty microliters of tissue extract was incubated with 200  $\mu$ L of substrate buffer consisting of 4.39 mL of 1.0 mol/L monobasic and 0.615 mL of 1.0 mol/L dibasic potassium phosphate, 83.3  $\mu$ L of 0.3%  $\text{H}_2\text{O}_2$ , and 0.834 mL of *ortho*-dianisidine HCl quantum sufficient to 50 mL with double distilled water. A plate reader was programmed to read optical density changes at 460 nm over a 2-minute period. MPO activities in samples were determined using a standard curve of purified MPO in the kit. Data are expressed as units of activity per gram of tissue.

#### Data Analysis

As there was no related literature, we performed a pilot study to obtain the mean values and SDs of the two major assays, Western blot of LC3 and TUNEL staining, in each group. According to the results of the pilot study, we estimated that the anticipated decreases of autophagy level as determined by Western blot of LC3 at 1, 6, 12, 24, 48, and 72 hours postburn versus normal level were 1.88, 3.46, 4.7, 4.34, 4.31, and 3.69 (optical density), respectively, and the anticipated increases of apoptotic rate as determined by TUNEL staining at 6, 24, 48, and 72 hours postburn versus normal level were 2.29, 8.81, 12.05, and 6.01%, respectively. The sample size was then obtained by using NCSS-PASS 11.0.4 software (NCSS, LLC, Kaysville, UT), assuming a significance level  $\alpha = 0.05$  and a power of test  $1 - \beta = 0.9$ .

Statistical analysis was undertaken using SPSS 18.0 software (IBM SPSS, Armonk, NY). Data are presented as means and standard errors ( $\pm$ SEs). The data from the control group were used for multiple comparisons with the experimental groups at each time point. Analysis of variance was used and multiple group comparisons were performed by using Dunnett's tests. Values of  $p < 0.05$  were considered statistically significant.

## RESULTS

#### Western Blot Analysis

Levels of LC3 and beclin-1 protein were maintained at a certain degree in normal skin tissue (normalized optical density, 3.69 [SE  $\pm$  0.07] and 0.67 [SE  $\pm$  0.01], respectively). After the burn was inflicted, levels of these proteins declined continuously in wound tissue until 24 hours after the burn. Levels then increased slightly, but remained significantly ( $p < 0.01$ ) lower than in normal skin samples. Quantitative analysis showed that autophagy levels decreased to one-fourth of normal level over 24 hours, and then gradually increased, but did not return to the normal baseline level during the 72-hour study (Figure 1).

#### TUNEL Assay

We found more cells undergoing apoptosis in burn wounds than controls. The mean apoptotic rates in burn wounds were 4.56% (SE  $\pm$  0.1%) at 6 hours, 11.76% (SE  $\pm$  0.25%) at 24 hours, 13.16% (SE  $\pm$  0.23%) at 48 hours, and 8.14% (SE  $\pm$  0.22%) at 72 hours versus 2.23% (SE  $\pm$  0.1%) of controls ( $p < 0.05$  at 6 hours;  $p < 0.01$  at 24, 48, and at 72 hours). The TUNEL-positive cells were mainly observed in the epithelium of hair follicles or blood vessels (Figures 2A-2D). Quantitative analysis demonstrated that TUNEL-positive cells in burn wounds were elevated about 3.7-fold over 48 hours and then decreased slightly, yet remained higher than in normal skin (Figure 2E).

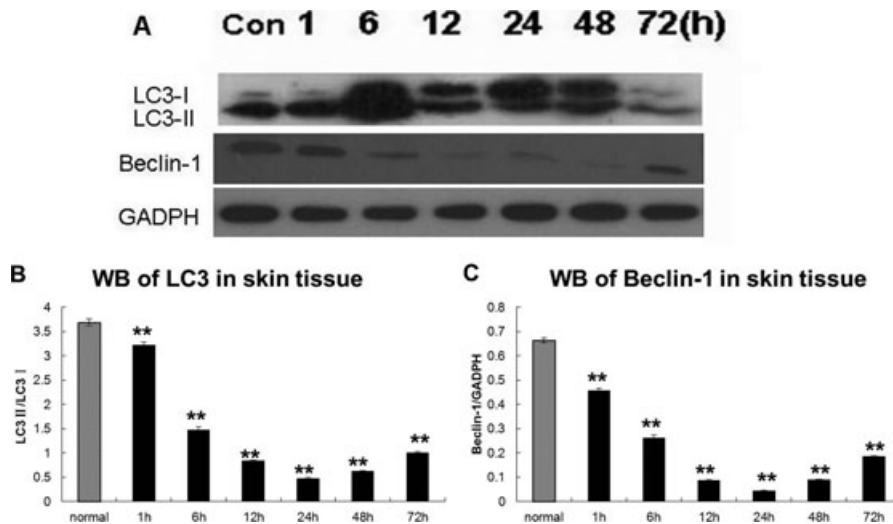


**Figure 1.** Western blot (WB) showing the expression of LC3 and beclin-1 protein in wound and normal tissue at different time points postburn (A). Expression of LC3II/I and beclin-1 in the burn wound tissue was lower than in normal skin (B, C). Data are presented as means  $\pm$  SE (burn vs. normal control, \* $p < 0.05$ , \*\* $p < 0.01$ ;  $n = 8$  per group). LC3 = Light Chain 3.

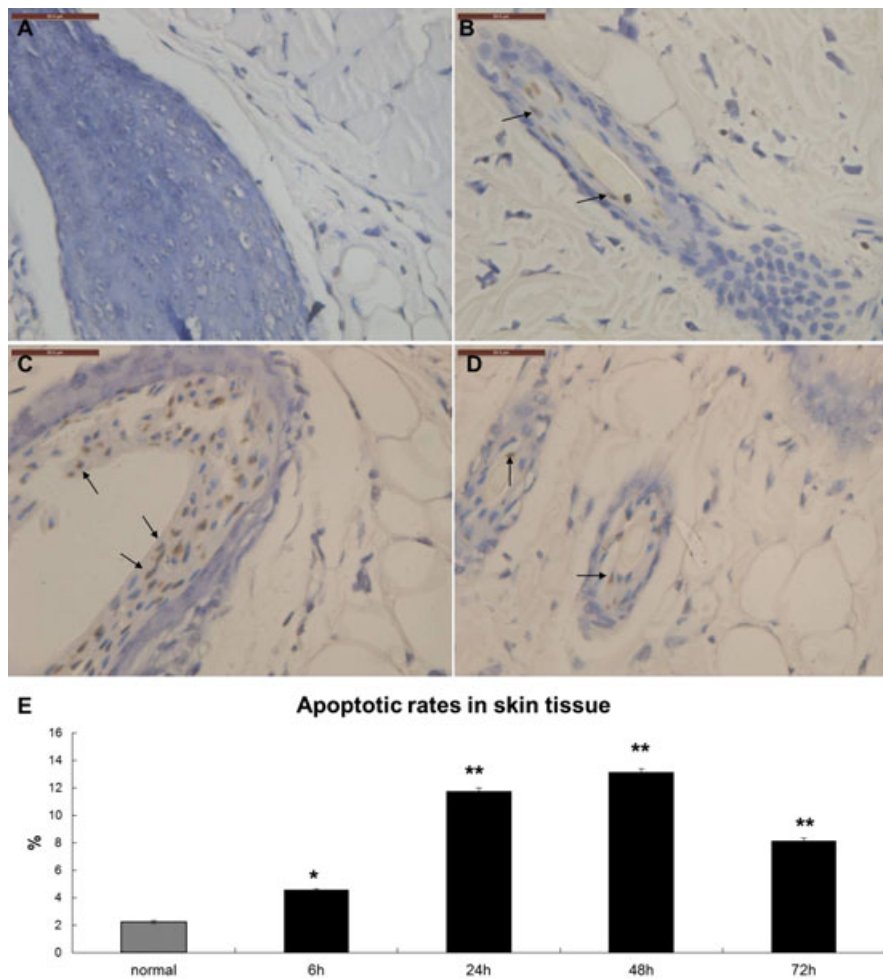


**Figure 2.** TUNEL staining of normal skin (A) and burn wound tissue 24 (B), 48 (C), and 72 (C) hours postburn. Cells with shrunken brown stained nuclei were considered positive (*black arrows*). The TUNEL-positive cells were mainly observed in the epithelium of hair follicles or blood vessels (A-D). Quantitative analysis demonstrated that TUNEL-positive cells in burn wounds were elevated about 3.7-fold over 48 hours and then decreased slightly, yet remained higher than in normal skin (E; *scale bars* = 50  $\mu$ m, burn vs. normal control, \* $p < 0.05$ , \*\* $p < 0.01$ ;  $n = 8$  per group). TUNEL = terminal-deoxynucleotidyl transferase mediated nick end labeling.

### H&E and Masson Staining

Histopathologic examination indicated that the burn wounds invaded progressively deeper levels of the skin as time progressed. At the 48- and 72-hour time points, there were fewer residual cutaneous appendages with more severe collagen denaturation, deeper tissue necrosis, and more profuse inflammatory infiltrates than at the 6-hour time point. Masson staining provided a good indicator of burn wound depth, and the boundary of the red dye defined the tissue necrosis boundary.<sup>16</sup> Deeper degrees of red coloration represented deeper penetration of the burn wound injury (Figure 3).

### Determination of LDF Value and MPO Activity

We found that blood flow, as measured by LDF values, decreased to one-fourth of normal level over the first 12 hours after injury and then began to rise but remained below ( $p < 0.01$ ) the baseline normal level. The MPO activity increased about 5.3-fold over the first 48 hours after injury and then decreased slightly, but still remained higher ( $p < 0.01$ ) than in normal tissue (Figure 4).

### Immunohistochemical Staining

Consistent with the results determined by Western blot assay, cells expressing LC3 in full-thickness wound tissues were significantly decreased as compared to controls (data not shown). By contrast, we found LC3-positive cells in the deep dermal layer adjacent to the subcutaneous tissue, which in this deep second-degree burn model may represent the zone of stasis, were much more than that of controls. In addition, we found that LC3-positive cells were mainly observed in the epithelium of hair follicles or macrophages (data not shown). Quantitative analysis demonstrated significant increases in LC3-positive cells in the deep dermis at 24 hours ( $p < 0.01$ ), 48 hours ( $p < 0.05$ ), and 72 hours ( $p < 0.01$ ) postburn (Figure 5).

## DISCUSSION

Burn wound progression continues to present practitioners with a complex and challenging clinical scenario. Previous research indicated that burn wounds were characterized by local perfusion deficiency, edema,

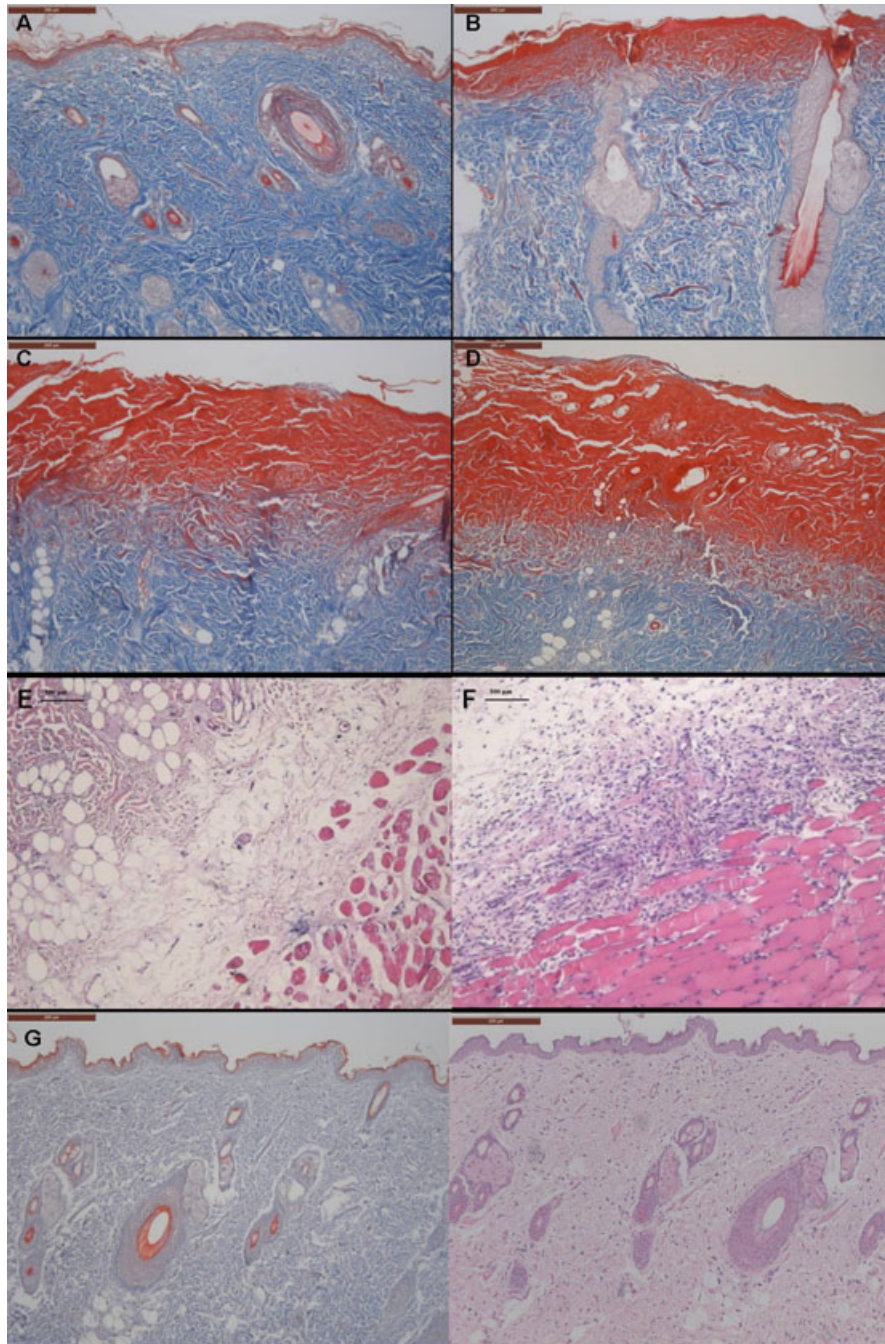


**Figure 3.** H&E and Masson staining of normal skin and burn wounds. Masson staining was a good indicator of burn wound depth. The red dye intensity reflects the tissue necrosis boundary.<sup>16</sup> The red dye intensity of burn wounds at 48 and 72 hours postburn (C, D) was markedly higher than that at 6 (A) and 24 hours postburn (B), indicating progression of wound depth with time. Fewer residual cutaneous appendages and more severe collagen denaturation were seen at 48 and 72 hours (C, D) than at 6 or 24 hours (A, B). H&E staining of burn wounds at 6 (E) and 48 hours postburn (F) showing more profuse inflammatory infiltrates at 48 hours. (G, H) Masson and H&E staining of normal skin. (A-D, G, H scale bars = 200  $\mu$ m; E, F scale bars = 100  $\mu$ m). H&E = hematoxylin and eosin.

thrombosis, free radical damage, accumulation of cell toxicity factors, and inflammatory infiltration, all of which contributed to wound deepening.<sup>3,17-19</sup> These factors are all thought to play an important role in burn wound progression, and previous studies have attempted, with variable success, to control burn wound deepening through interventions that counteract these mechanisms.<sup>17,19,20</sup>

More recent studies have centered on investigating the role of apoptosis and necrosis in burn wound progression. It has been reported that the rate of cell apoptosis in deep second-degree burn wounds is much higher than in normal skin of burn patients, which indicates that apoptosis may be involved in burn wound progression.<sup>4</sup> Furthermore, prevention of apoptotic cell death in burn wounds can reduce dermal tissue loss

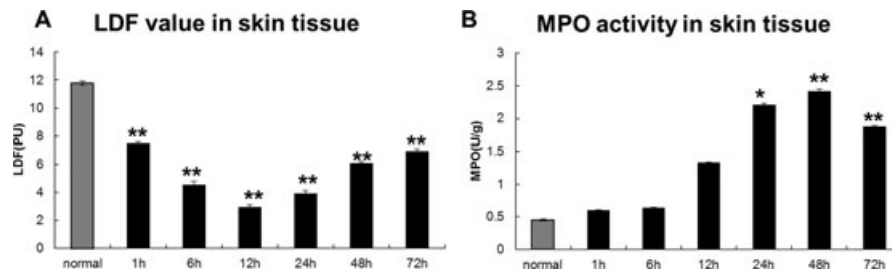


**Figure 4.** LDF values and MPO activity in burn wounds and normal skin. (A) LDF values in the burn wounds were significantly decreased compared to the control group. LDF values in the burn wounds decreased to one-fourth of normal level over 12 hours and then began to rise but remained below ( $p < 0.01$ ) the baseline normal level. (B) MPO activities in burn wounds were significantly increased compared with the control. The levels of MPO activity in burn wounds were increased 5.3-fold over 48 hours and then decreased but were still far higher ( $p < 0.01$ ) than in normal tissue. Alterations in the LDF value were significant at all the time points postburn. Changes in the levels of MPO activity between burn and control groups were significant at the time points of 24, 48, and 72 hours postburn. The values described herein were mean  $\pm$  SE (burn vs. control group, \* $p < 0.05$ , \*\* $p < 0.01$ ,  $n = 8$  per group). LDF = laser Doppler flowmetry; MPO = myeloperoxidase.

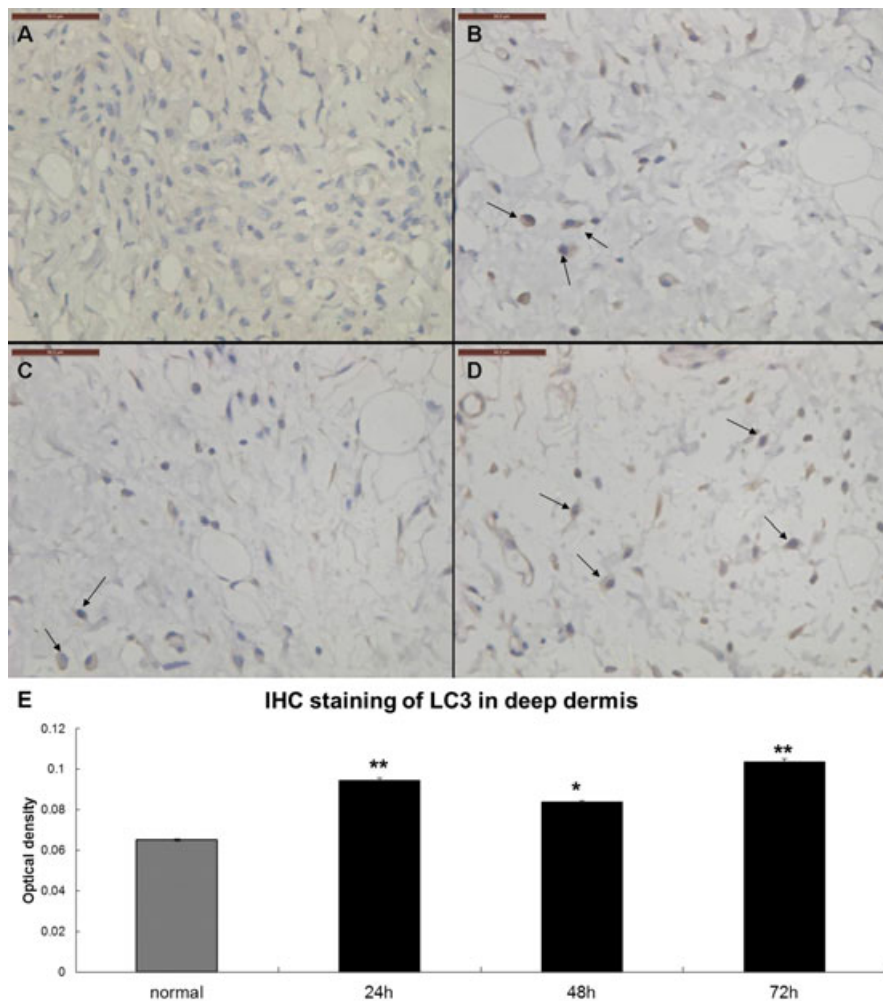


**Figure 5.** IHC staining of LC3 (black arrows, cells with brown cytoplasm) in the deep dermis of normal skin (A) and burn wounds (B-D). (B) 24 hours postburn; (C) 48 hours postburn; (D) 72 hours postburn. At all time points after burn, the cells expressing LC3 were increased in the deep dermis of burn wound tissue compared to that of control. Scale bars = 50  $\mu$ m. (E) Quantitative analysis of the immunohistochemical staining showed that the expression of LC3 in the deep dermis of burn wounds was significantly higher than that of the control at all time points ( $p < 0.01$  at 24 and 72 hours;  $p < 0.05$  at 48 hours postburn). The values herein were mean  $\pm$  SE (burn vs. normal control, \* $p < 0.05$ , \*\* $p < 0.01$ ,  $n = 8$  per group). IHC = immunohistochemical; LC3 = Light Chain 3; LDF = laser Doppler flowmetry.

and promote wound healing.<sup>6,7</sup> Cellular apoptosis plays an important role in maintaining homeostasis, cell differentiation, and development; in fighting against pathogens; and in the removal of inflammatory cells.<sup>21,22</sup> However, in models of myocardial ischemia, cellular apoptosis was found to aggravate ischemic damage, while reducing apoptosis reduced ischemic injury.<sup>23</sup> It seems likely that the increase of apoptosis exacerbated the ischemic damage within the deep dermal zone of burn wounds and thus participated in the burn wound progression.

Autophagy is a highly conserved pathway that delivers intracellular macromolecule waste to lysosomes, where they are degraded into biologically active monomers, such as amino acids, that are subsequently reused to maintain cellular metabolic turnover and homeostasis.<sup>9</sup> Autophagy principally serves an adaptive role to protect organisms against diverse insults, including infection, cancer, neurodegeneration, aging, and heart disease. Defects in the process of autophagy have been closely related to neurodegenerative disease, cardiomyopathy, diabetes, fatty liver disease, and Crohn's disease.<sup>24–26</sup> Enhancement of autophagic activity has been shown to protect against myocardial ischemia–reperfusion injury,<sup>27</sup> reduce neuronal ischemic anoxia injury,<sup>28</sup> slow down the process of aging, and protect against many diseases.<sup>29</sup>

There are few published articles describing the relationship between autophagy and burn wound progression. It is well known that autophagy plays dual roles in cell survival and cell death.<sup>30–32</sup> During nutrient deprivation, ischemia, or inflammation,<sup>33</sup> autophagy is activated and has a cytoprotective role, but several stress stimuli can induce autophagy and, thus, distinct programmed cell death pathways can be activated when stress is not abolished.<sup>34</sup> It would be intriguing to know whether autophagy plays a prosurvival or prodeath role in the pathophysiology of burn injury progression.

In our study, the autophagy level was at first reduced and then increased, yet remained far below that in normal skin. We speculate that at the early stage of burn wound progression the number of cells undergoing autophagy is reduced as cellular necrosis becomes the predominant activity. At the latter stage, when the inevitable tissue necrosis ceased, the remaining viable tissue adjacent to coagulation was subject to ischemic and inflammatory damage among others, and then autophagy might serve to protect against these stress stimuli as a survival mechanism, which accounts for the later rise in the levels of autophagy. The prosurvival role of autophagy is supported by IHC staining that demonstrated significantly activated autophagy in the deep dermis, which in this burn model represents the zone of stasis (or ischemia). In addition, at the later stage (48 to 72 hours after burn injury), tissue perfusion was restored and inflammation was reduced in parallel with the increased levels of autophagy, which supports the prosurvival role of autophagy in this burn model. It is important to stress that the estimates of cutaneous blood flow obtained using LDF in this study are not absolute measurements of this parameter and may be affected by different instruments or anesthetics, among other possible variables. Since the same instrument,

detecting techniques, and anesthetics were used for both groups, the comparison of relative blood flow between groups is valid. The data obtained should be used to estimate relative differences between groups and not as absolute point estimates.

Apoptosis interfaces with autophagy in many different ways, which are as complicated as autophagy's ambiguous roles in life and death. Some suggest that autophagy is a trigger for apoptotic cell death,<sup>35,36</sup> while others argue that autophagy protects against apoptosis and inflammation.<sup>37–39</sup> In this study, the apoptotic rates determined by TUNEL assay in burn wounds rose at first and then declined after 48 hours postburn, which is almost completely contrary to the changes in the levels of autophagy. These findings may indicate the complementary roles of autophagy and apoptosis in this model of burn wound progression. However, further study is still needed to confirm these hypotheses, and the underlying cellular and molecular mechanisms involved in this process urgently need to be disclosed.

## LIMITATIONS

---

Our study is limited by its small sample size and relatively short follow-up period. Furthermore, the study is also limited to rats and cannot necessarily be generalized to other, larger species. There was no attempt to correlate the study findings with longer-term healing endpoints such as reepithelialization and scarring. Further study is still needed to demonstrate if enhanced or decreased autophagy, through intervening measures, would alter apoptosis rate, burn wound progression, and wound healing.

## CONCLUSIONS

---

Our study demonstrated reduced levels of autophagy and blood flow together with increased levels of inflammation and apoptosis during the early course of burn wound progression in a rodent model. These findings suggest that autophagy and apoptosis play complementary roles in the process of burn progression. Enhanced autophagy in the deep dermal layers may function as a prosurvival mechanism against inflammation and ischemia.

## References

---

1. Singh V, Devgan L, Bhat S, Milner SM. The pathogenesis of burn wound conversion. *Ann Plastic Surg* 2007;59:109–15.
2. Shupp JW, Nasabzadeh TJ, Rosenthal DS, Jordan MH, Fidler P, Jeng JC. A review of the local pathophysiologic bases of burn wound progression. *J Burn Care Res* 2010;31:849–73.
3. Kao CC, Garner WL. Acute burns. *Plastic Reconstr Surg* 2000;101:2482–93.
4. Gravante G, Palmieri MB, Esposito G, et al. Apoptotic death in deep partial thickness burns vs. normal skin of burned patients. *J Surg Res* 2007;141:141–5.
5. Singer AJ, McClain SA, Taira BR, Guerriero JL, Zong W. Apoptosis and necrosis in the ischemic zone adjacent to third degree burns. *Acad Emerg Med* 2008;15:549–54.



6. Giles N, Rea S, Beer T, Wood FM, Fear MW. A peptide inhibitor of c-Jun promotes wound healing in a mouse full-thickness burn model. *Wound Repair Regen* 2008;16:58–64.
7. Ipaktchi K, Mattar A, Niederbichler AD, et al. Topical p38MAPK inhibition reduces dermal inflammation and epithelial apoptosis in burn wounds. *Shock* 2006;26:201–9.
8. Reggiori F, Klionsky DJ. Autophagy in the eukaryotic cell. *Eukaryot Cell* 2002;1:11–21.
9. Shintani T, Klionsky DJ. Autophagy in health and disease: a double-edged sword. *Science* 2004;306:990–5.
10. Yuhua S, Ligen L, Jiake C, Tongzhu S. Effect of Poloxamer 188 on deepening of deep second-degree burn wounds in the early stage. *Burns* 2012;38:95–101.
11. Lang T, Schaeffeler E, Bernreuther D, Bredschneider M, Wolf DH, Thumm M. Aut2p and Aut7p, two novel microtubule-associated proteins are essential for delivery of autophagic vesicles to the vacuole. *EMBO J* 1998;17:3597–607.
12. Ichimura Y, Kirisako T, Takao T, et al. A ubiquitin-like system mediates protein lipidation. *Nature* 2000;408:488–92.
13. Kabeya Y, Mizushima N, Yamamoto A, Oshitani-Okamoto S, Ohsumi Y, Yoshimori T. LC3, GABARAP and GATE16 localize to autophagosomal membrane depending on form-II formation. *J Cell Sci* 2004;117:2805–12.
14. Kametaka S, Okano T, Ohsumi M, Ohsumi Y. Apg14p and Apg6/Vps30p form a protein complex essential for autophagy in the yeast, *Saccharomyces cerevisiae*. *J Biol Chem* 1998;273:22284–91.
15. Tu SP, Quante M, Bhagat G, et al. IFN-gamma inhibits gastric carcinogenesis by inducing epithelial cell autophagy and T-cell apoptosis. *Cancer Res* 2011;71:4247–59.
16. Lu S, Xiang J, Jin S, et al. Histological observation of the effects of tangential excision within twenty-four postburn hours on the progressive injury of the progression of deep partial thickness burn wound [Chinese]. *Zhonghua Shao Shang Za Zhi* 2002;18:235–7.
17. Barrow RE, Ramirez RJ, Zhang XJ. Ibuprofen modulates tissue perfusion in partial-thickness burns. *Burns* 2000;26:341–6.
18. Baskaran H, Yarmush ML, Berthiaume F. Dynamics of tissue neutrophil sequestration after cutaneous burns in rats. *J Surg Res* 2000;93:88–96.
19. Mahajan AL, Tenorio X, Pepper MS, et al. Progressive tissue injury in burns is reduced by rNAPc2. *Burns* 2006;32:957–63.
20. Baskaran H, Toner M, Yarmush ML, Berthiaume F. Poloxamer-188 improves capillary blood flow and tissue viability in a cutaneous burn wound. *J Surg Res* 2001;101:56–61.
21. Renahan AG, Booth C, Potten CS. What is apoptosis, and why is it important? *BMJ* 2001;322:1536–8.
22. Opferman JT, Korsmeyer SJ. Apoptosis in the development and maintenance of the immune system. *Nature Immunol* 2003;4:410–5.
23. Hochhauser E, Kivity S, Offen D, et al. Bax ablation protects against myocardial ischemia-reperfusion injury in transgenic mice. *Am J Physiol Heart Circ Physiol* 2003;284:H2351–9.
24. Levine B, Kroemer G. Autophagy in the pathogenesis of disease. *Cell* 2008;132:27–42.
25. Eskelinen EL, Saftig P. Autophagy: a lysosomal degradation pathway with a central role in health and disease. *Biochim Biophys Acta* 2009;1793:664–73.
26. Virgin HW, Levine B. Autophagy genes in immunity. *Nature Immunol* 2009;10:461–70.
27. Nishida K, Kyoji S, Yamaguchi O, Sadoshima J, Otsu K. The role of autophagy in the heart. *Cell Death Differ* 2009;16:31–8.
28. Bae N, Ahn T, Chung S, et al. The neuroprotective effect of modified Yeoldahanso-tang via autophagy enhancement in models of Parkinson's disease. *J Ethnopharmacol* 2011;134:313–22.
29. Mizushima N, Levine B, Cuervo AM, Klionsky DJ. Autophagy fights disease through cellular self-digestion. *Nature* 2008;451:1069–75.
30. Baehrecke EH. Autophagy: dual roles in life and death? *Nat Rev Mol Cell Biol* 2005;6:505–10.
31. Eskelinen EL. The dual role of autophagy in cancer. *Curr Opin Pharmacol* 2011;11:294–300.
32. Kang C, You YJ, Avery L. Dual roles of autophagy in the survival of *Caenorhabditis elegans* during starvation. *Genes Dev* 2007;21:2161–71.
33. Levine B, Mizushima N, Virgin HW. Autophagy in immunity and inflammation. *Nature* 2011;469:323–35.
34. Thome RG, Santos HB, Arantes FP, Domingos FF, Bazzoli N, Rizzo E. Dual roles for autophagy during follicular atresia in fish ovary. *Autophagy* 2009;5:117–9.
35. Shrivastava A, Kuzontkoski PM, Groopman JE, Prasad A. Cannabidiol induces programmed cell death in breast cancer cells by coordinating the cross-talk between apoptosis and autophagy. *Mol Cancer Ther* 2011;10:1161–72.
36. Nezis IP, Shrivastava BV, Sagona AP, Johansen T, Baehrecke EH, Stenmark H. Autophagy as a trigger for cell death: autophagic degradation of inhibitor of apoptosis dBruce controls DNA fragmentation during late oogenesis in *Drosophila*. *Autophagy* 2010;6:1214–5.
37. Zou MH, Xie Z. Regulation of interplay between autophagy and apoptosis in the diabetic heart: new role of AMPK. *Autophagy* 2013;9:624–5.
38. Zeng R, He J, Peng J, et al. The time-dependent autophagy protects against apoptosis with possible involvement of Sirt1 protein in multiple myeloma under nutrient depletion. *Ann Hematol* 2012;91:407–17.
39. Xi G, Hu X, Wu B, et al. Autophagy inhibition promotes paclitaxel-induced apoptosis in cancer cells. *Cancer Lett* 2011;307:141–8.